

A First-Principles Study on the Structural and Electronic Properties of C₃₆ Molecules

Lan-Feng Yuan, Jinlong Yang,* Ke Deng, and Qing-Shi Zhu

Open Laboratory of Bond Selective Chemistry, University of Science and Technology of China, Hefei, Anhui 230026, P.R. China

Received: March 15, 2000

The structural and electronic properties of C₃₆ molecules with two most possible geometries (D_{2d} and D_{6h}) are studied using the Hartree–Fock (HF), density functional theory (DFT) with the local density approximation (LDA) and generalized gradient approximation (GGA), and hybrid DFT methods. The results show that the ground state of the D_{6h} isomer strongly depends on the computational methods. The HF and hybrid DFT predict a triplet ground state, whereas the LDA and GGA give a singlet one. The D_{2d} and D_{6h} isomers are quasi-isoenergetic at their ground states. Our results indicate that the relative stability of the two isomers can be alternated by gaining or losing an electron. The D_{6h} anion is more stable than the D_{2d} anion, whereas the D_{2d} cation is lower in energy than the D_{6h} cation. These results are used to understand the experimental fact that the C₃₆ molecule in the solid has D_{6h} symmetry and to predict the possible D_{2d} C₃₆ molecules, ions, and solids. The vibrational frequencies, ionization potentials, electron affinities, energy gaps, and molecular densities of states are obtained for the two isomers. The results are discussed and compared with the available experimental results.

Introduction

Since the discovery¹ and macroscopic scale synthesis² of C₆₀, the fullerenes have attracted extensive scientific interest because of their novel and unusual physical and chemical properties. Most researchers focused mainly on C₆₀, C₇₀, and some larger fullerenes. The bulk synthesis of C₃₆ suggests that this situation may be about to change. Piskoti et al.³ synthesized C₃₆ crystal by the arc-discharge method, which is the first time that a fullerene smaller than C₆₀ has been produced in a large scale. The C₃₆ molecule is far more chemically reactive than C₆₀. This fullerene and its derivatives are believed to make a class of promising materials with new structural and electronic properties, such as covalent bonding, high reactivity, significant steric strain, low gap, high strength, and superconductivity.^{4–6} So, scientific interest in the C₃₆ fullerene has been growing very rapidly.

Various experimental techniques have been employed to study the structural and electronic properties of C₃₆. Piskoti et al.³ reported a solid-state nuclear magnetic resonance (NMR) measurement on a C₃₆ solid and suggested that the C₃₆ molecule has D_{6h} symmetry. Kietzmann et al.⁷ recorded the photoelectron spectrum (PES) of the C₃₆ anion and derived that the C₃₆ molecule exhibits a gap of 0.8 eV with a large experimental error bar. Collins et al.⁸ measured the scanning tunneling spectra (STS) of C₃₆ islands and obtained sharp features in the density of states (DOS) and an 0.8 eV electronic gap.

On the theoretical side, Grossman et al.⁹ investigated six likely isomers of molecular C₃₆ using density functional theory (DFT) with both the local density and generalized gradient approximations (LDA and GGA, respectively). They predicted the D_{6h} and D_{2d} fullerenes to be the most energetically favorable structures and to be essentially isoenergetic. Slanina et al.¹⁰ searched the lowest energy structure of C₃₆ through 598 cages by the SAM1 semiempirical method and concluded that the D_{2d}

isomer has the lowest energy. Halac et al.¹¹ explored three possible structures of C₃₆ using a semiempirical covalent potential and showed that the D_{6h} structure is the most stable, whereas the D_{2d} structure is very close to it in energy. Fowler et al.¹² optimized a total of 15 classical and 73 nonclassical C₃₆ fullerenes using the density-functional tight binding (DFTB), QCFF/PI, MNDO and its variants AM1 and PM3 methods. They found that the D_{2d} structure is always the lowest in energy and the energy difference between the D_{2d} and D_{6h} structures depends strongly on the computational methods, ranging from 0.12 to 1.63 eV. Jagadeesh et al.¹³ studied the triplet state of the D_{6h} isomer, which was not explicitly considered in previous calculations. They optimized the structures at the AM1 and Hartree–Fock (HF) levels and performed additional computations with the hybrid DFT method. Their results indicate that the D_{6h} isomer prefers a triplet ground state and is the lowest-energy structure for C₃₆.

All the efforts just described are helpful in understanding the structural and electronic properties of C₃₆, but there are still some fundamental and important issues to be clarified. First, what is the ground state of the two isomers? The conclusion of Jagadeesh et al.¹³ needs to be checked using more reliable procedures. Second, are the D_{2d} and D_{6h} isomers isoenergetic? The conflicting results just stated clearly motivate more studies on this question. Third, if the D_{2d} and D_{6h} isomers are isoenergetic, how can one understand the experimental fact³ that the C₃₆ molecule in the solid is of D_{6h} symmetry?

In this paper, we perform a comprehensive first-principles study on C₃₆ molecules with two most possible geometries (D_{2d} and D_{6h}, shown in Figure 1) in the hope of clarifying these issues.

Computational Details

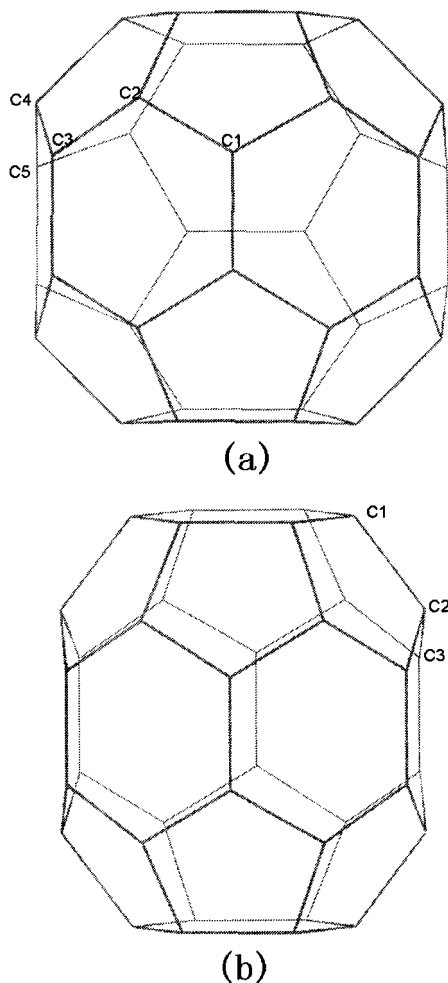
We use five ab initio methods, as implemented in the Gaussian 94 package,¹⁴ to study the isomers (i.e., the HF, LDA,

* Corresponding author. E-mail: jlyang@ustc.edu.cn.

TABLE 1: Energy Differences (eV) for the Two C₃₆ Isomers Within the HF, LDA (VWN), GGA (PW91), B3LYP, and B3PW91 Methods, Relative to the Singlet State of the D_{6h} Isomer^a

isomer	energy difference (eV)									
	HF	LDA	GGA	B3LYP	B3PW91	ref 9	ref 10	ref 11	ref 12	ref 13
D _{6h} singlet	0.00	0.00	0.00	0.00	0.00	0.00	0.00	0.00	0.00	0.00
D _{6h} triplet	-2.35	0.27	0.26	-0.16	-0.18					-0.21
D _{2d} singlet	-1.12	0.03	0.06	-0.16	-0.13	0.00	-1.39	0.14	-0.12	-1.63
D _{2d} triplet	-1.22	0.52	0.56	0.17	0.15					0.03
										85

^a Each structure has been fully relaxed within the given symmetry by all the methods.

**Figure 1.** Geometries of C₃₆: (a) the D_{2d} isomer; (b) the D_{6h} isomer.

GGA, B3LYP, and B3PW91 methods). The Vosko–Wilk–Nusair parameterization¹⁵ of the local exchange–correlation energy is used in LDA, and the Perdew–Wang parameterization¹⁶ of the gradient-corrected exchange–correlation energy is used in GGA. The B3LYP and B3PW91 are two hybrid DFT methods where the exchange potentials include pure DFT exchange functionals plus the exact HF exchange, with three parameters adjusted according to some experimental values of a few selected compounds. The B3LYP employs the Becke exchange gradient correction¹⁷ with the Lee, Yang, and Parr gradient-corrected correlation energy functional,¹⁸ and B3PW91 with the Perdew–Wang gradient-corrected correlation.¹⁶ All calculations are carried out with (50,194) pruned grid (containing ~3600 points per atom) and 6-31G(d) basis set.¹⁹

Results and Discussion

A. Energies and Geometries of Two Molecular Isomers.

We first perform geometry optimizations on the singlet and

TABLE 2: Optimized C–C Bond Lengths (Å) in the D_{6h} Isomers at the Ground States

bond	bond length (Å)						
	HF	LDA	GGA	B3LYP	B3PW91	ref 9	ref 11
C1–C1	1.393	1.407	1.404	1.412	1.409	1.41	1.46
C1–C2	1.487	1.476	1.470	1.489	1.484	1.48	1.49
C2–C3	1.421	1.424	1.420	1.432	1.428	1.43	1.47
C3–C3	1.447	1.431	1.427	1.446	1.443	1.43	1.43

triplet states of the two isomers using the five methods. The results are listed in Table 1. A striking result is that the ground state of the D_{6h} isomer depends strongly on the computational methods. At the HF, B3LYP, and B3PW91 levels, the ground state of the D_{6h} isomer is the triplet state, whereas at the LDA and GGA levels it is the singlet state. This observation agrees implicitly with the biradicaloid nature of the singlet state predicated by Fowler et al.⁵ Our LDA and GGA results repeat those of Grossman et al.⁹ Recently, however, the hybrid DFT is believed to be more precise than the LDA and GGA methods. If one agrees with this judgement, our results indicate the ground state of the D_{6h} isomer is the triplet one, which is in agreement with the results of Jagadeesh et al.¹³ The ground state of the D_{2d} isomer is the singlet state as determined by all the methods except HF. This result agrees with all the previous calculations.^{9–13} Comparing the ground-state energy of the D_{2d} isomer with that of the D_{6h} isomer in Table 1, one can find that the difference between them is very small (<0.06 eV) for all the methods except the HF. The HF method predicts that the triplet state of the D_{6h} isomer is much lower in energy (1.23 eV) than the singlet state of the D_{2d} isomer. We think this result is unreliable because the HF method does not consider the electronic correlation effect. The electronic correlation effect has been proved to be important in C₆₀,^{20,21} and we believe it is also significant in C₃₆. Thus, the two isomers can be viewed to be quasi-isoenergetic. This conclusion is in contrast with that of Jagadeesh et al.¹³ The discrepancy, we believe, arises because of the simplification in their calculations; that is, Jagadeesh et al.¹³ only optimized the geometries of C₃₆ with the semiempirical AM1 hamiltonian and ab initio HF procedure with the split-valence 3-21G basis set.

The optimized C–C bond lengths in the two isomers at their ground states are listed for the five methods in Tables 2 and 3. All the methods give quite similar values. As shown in Figure 1, both the isomers consist of 12 pentagons and 8 hexagons. In the D_{6h} isomer, there are three sets of nonequivalent atoms and four kinds of C–C bonds. If we take the bond lengths of typical C–C single bonds (1.54 Å in ethane) and double bonds (1.34 Å in ethene) as references, we can view approximately the C1-to-C2 and C1-to-C1 bonds in the D_{6h} isomer as the single and double bonds, respectively. It is difficult to define the C2-to-C3 and C3-to-C3 bonds as single or double because their lengths lie just at the middle of the single and double bond lengths. This result is different from that of C₆₀ where only two kinds of C-to-C bonds exist; they are, the so-called single bonds (1.45 Å) and double bonds (1.40 Å). A similar analysis can be applied

TABLE 3: Optimized C—C Bond Lengths (Å) in the D_{2d} Isomers at the Ground State

method	bond length (Å)								
	C1-C1	C1-C2	C2-C3	C3-C3	C2-C5	C5-C5	C3-C4	C4-C5	C4-C4
HF	1.425	1.428	1.395	1.434	1.487	1.429	1.470	1.352	1.479
LDA	1.430	1.431	1.422	1.440	1.464	1.416	1.446	1.390	1.467
GGA	1.425	1.427	1.418	1.436	1.458	1.414	1.440	1.388	1.462
B3LYP	1.440	1.438	1.424	1.449	1.482	1.425	1.461	1.388	1.482
B3PW91	1.437	1.435	1.421	1.445	1.476	1.422	1.456	1.386	1.477

TABLE 4: Energy Differences (eV) for the Anionic and Cationic C_{36} Isomers Within the HF, LDA (VWN), GGA (PW91), B3LYP, and B3PW91 Methods Relative to the D_{6h} anion^a

isomer		energy difference (eV)				
		HF	LDA	GGA	B3LYP	B3PW91
anionic	D_{6h}	0.00	0.00	0.00	0.00	0.00
	D_{2d}	-0.17	0.26	0.29	0.19	0.21
cationic	D_{6h}	7.44	10.75	9.56	9.20	9.57
	D_{2d}	6.65	10.47	9.33	8.91	9.29

^a Because of the existence of the Jahn–Teller effect in the D_{2d} anion, its geometry optimizations have been performed without the symmetry constraint.

to the D_{2d} results in Table 3. In a word, the diffuse distribution of C-to-C bond lengths in C_{36} implies complicated C-to-C bondings.

B. Energies of Ionic Isomers. We have just shown that the D_{2d} and D_{6d} isomers are quasi-isoenergetic, which means they might have equal chances to appear in C_{36} solids. This inference obviously conflicts with the experimental fact³ that the molecules in the C_{36} solid are of D_{6h} symmetry. It is unlikely that the D_{2d} isomers will transform to the D_{6h} ones when they form the solid with the superiority of the crystalline lattice stabilization energy of the D_{6h} isomers because this process will accompany the breaking of the C-C bonds. To explain this discrepancy, we notice that the synthesis of the C_{36} solid is achieved by the arc-discharge method where the C_{36} ions might be first formed and then the solid appears. Therefore, the stability of the ionic isomers rather than that of the neutral isomers might determine the molecular geometries in the C_{36} solid.

We optimize the geometries of the anionic and cationic isomers. The relative energies at their equilibrium configurations are listed in Table 4. The results indicate that all the methods except the HF predict the anionic D_{6h} isomer is more stable than the anionic D_{2d} one. The energy difference between these isomers is as large as ~ 0.2 eV. If we assume that in the arc-discharge process the carbon atoms and ions first form the C_{36} anions and then the anions are aggregated to form the solid by losing extra electrons to the substrate, our result implies the C_{36} solid will be made of the D_{6h} isomers which is in agreement with the experimental fact of Piskoti et al.³ Our explanation is the first likely one for the experimental fact³ that the molecules in the C_{36} solid are of D_{6h} symmetry and is supported by a very recent study of the reaction pathway for the formation of a C_{36} dimer.²² Grossman et al.²² predicted that the reaction pathway to form a neutral C_{36} dimer is barrierless, whereas negatively charged C_{36} molecules are less likely to bond because of a substantial barrier of formation. They proposed that it may be necessary and desirable to provide a source of negative ions to form the C_{36} solid. Certainly, we should point out that our explanation is based on the thermodynamical analysis only and the mechanism of formation of C_{36} might be very complex and more further studies are needed.

From the data in Table 4, one can also see that the cationic D_{2d} isomer is more stable than the cationic D_{6h} for all the

TABLE 5: IR Active Modes Frequencies (cm^{-1}) (Intensities in Parenthesis; arbitrary unit) of the D_{2d} and D_{6h} Isomers

	D_{2d}		D_{6h}	
	B_2	E	A_{2u}	E_{1u}
	362 (0.514)	261 (18.9)	490 (110)	447 (5.32)
	474 (0.420)	406 (0.47)	714 (163)	475 (14.4)
	594 (0.446)	476 (8.33)	786 (6.58)	640 (17.2)
	690 (0.207)	501 (3.07)	1112 (53.1)	730 (21.7)
	706 (7.57)	544 (7.09)	1349 (0.55)	1092 (16.8)
	719 (19.8)	599 (0.52)		1276 (7.30)
	922 (1.28)	656 (0.81)		1366 (40.0)
	1139 (0.01)	676 (6.18)		1479 (25.3)
	1286 (20.7)	693 (0.85)		
	1317 (9.10)	703 (7.41)		
	1431 (3.54)	717 (26.5)		
	1463 (1.22)	750 (11.4)		
	1570 (1.22)	773 (0.46)		
		950 (4.29)		
		1105 (0.70)		
		1143 (0.82)		
		1207 (5.63)		
		1225 (0.02)		
		1276 (12.5)		
		1295 (0.07)		
		1329 (20.6)		
		1402 (18.8)		
		1457 (0.02)		
		1513 (33.4)		
		1521 (0.34)		

methods. With this result, one can conceive that if there are any physical or chemical means by which the cations appear first, the D_{2d} C_{36} molecules, ions, and possible solids might be synthesized.

C. Vibrational Frequencies and Geometric Stability. To verify whether the D_{2d} and D_{6h} molecular isomers are local minima in the potential energy surface and to understand the experimental infrared (IR) spectrum,³ frequency calculations for the two isomers are performed at the LDA level. Symmetry analysis of the vibrational modes leads to the following decompositions: $\Gamma_{D_{2d}} = 14A_1 + 12A_2 + 13B_1 + 13B_2 + 25E$, and $\Gamma_{D_{6h}} = 6A_{1g} + 2A_{2g} + 5B_{1g} + 4B_{2g} + 8E_{1g} + 9E_{2g} + 3A_{1u} + 5A_{2u} + 4B_{1u} + 5B_{2u} + 8E_{1u} + 9E_{2u}$ (the σ_d planes pass through the C3–C3 bonds). Among them, the B_2 and E modes of the D_{2d} isomer and the A_{2u} and E_{1u} modes of the D_{6h} isomer are IR active, whereas the A_1 , B_1 , B_2 , and E modes of the D_{2d} isomer and the A_{1g} , E_{1g} , and E_{2g} modes of the D_{6h} isomer are Raman active. In Tables 5, 6, and 7 are shown the IR active, Raman active, and silent modes frequencies of the two isomers. Our calculated frequencies are all positive for the two isomers, so we conclude that the two isomers are indeed local minima. Symmetry reduction was previously suggested for C_{36} molecules; for example, $D_{6h} \rightarrow C_{6v}$ distortion due to the second-order Jahn–Teller effect.¹² However, we notice that the second-order Jahn–Teller effect is not a rigid principle but just provides a proposal.^{23,24} Furthermore, the symmetry change from D_{6h} to C_{6v} should cause transparent consequences for its ¹³C NMR spectrum,¹² which is not the case of the experimental result.³ Our calculated frequencies of the D_{6h} isomer are compatible

TABLE 6: Raman Active Modes Frequencies (cm⁻¹) of the D_{2d} and D_{6h} Isomers^a

D _{2d}		D _{6h}		
A ₁	B ₁	A _{1g}	E _{1g}	E _{2g}
333	272	368	339	293
455	493	630	538	551
480	524	730	704	603
559	652	926	714	641
634	684	1241	970	971
719	718	1555	1257	1149
954	779		1340	1293
1117	965		1466	1459
1178	1249			1542
1262	1276			
1348	1279			
1406	1427			
1481	1531			
1545				

^a The Raman active B₂ and E modes of the D_{2d} isomer are also IR active and listed in Table 5.

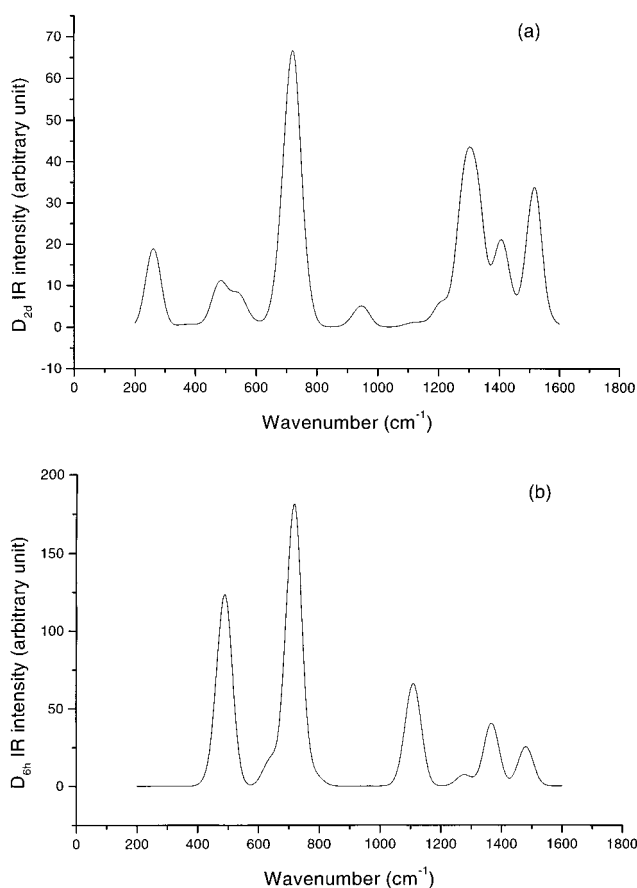
TABLE 7: Silent Modes Frequencies (cm⁻¹) of the D_{2d} and D_{6h} Isomers

D _{2d}		D _{6h}					
A ₂	A _{2g}	B _{1g}	B _{2g}	A _{1u}	B _{1u}	B _{2u}	E _{2u}
408	714	553	624	396	440	430	448
437	1434	623	702	727	1167	671	533
543		830	1376	1299	1421	730	639
645		1262	1425		1478	1161	734
711		1276				1268	799
751							1138
835							1228
1130							1462
1250							1530
1268							
1461							
1509							

with those by Jishi and Dresselhaus.²⁵ They also found that the frequencies of the D_{6h} isomer with charge number from -2 to 2 are all positive,²⁵ corresponding to the convergent behavior of our D_{6h} ionic states. We find out the Jahn-Teller distortion of the D_{2d} anion and its optimization has been performed without the symmetric constraint. Our calculation for the D_{2d} cation is convergent, and even if there exists a distorted state with lower symmetry and lower energy, our conclusion that in the cationic state the D_{2d} isomer is more stable than the D_{6h} isomer would not change.

The theoretical IR transmission spectra of two isomers are obtained by a Gaussian extension of the IR active lines and a summation over them (see Figure 2). The broadening width is set as 25 cm⁻¹. The room temperature mid-IR transmission spectrum for C₃₆ powder dispersed in KBr had been obtained by Piskoti et al.³ Comparing our calculated spectra with the experimental one, it can be seen that the experimental spectrum is very similar to the theoretical D_{6h} spectrum and the two theoretical spectra can be distinguished. The difference between the experimental and theoretical D_{6h} spectra indicates the influence of intermolecular correlation in solids.

D. Electronic Properties. The adiabatic and vertical ionization potentials (IPs) and electron affinities (EAs) for the two isomers are listed in Table 8. We define two types of vertical IPs and EAs. In type I, the total energies of the neutral and ionic isomers are calculated at the optimized molecular geometries, and in type II, they are calculated at the optimized ionic geometries. The IPs and EAs given by the GGA, B3LYP, and B3PW91 methods are quite close. These values are very different from those determined by the HF and LDA methods.

**Figure 2.** The calculated IR emission spectra of C₃₆ by LDA: (a) the D_{2d} isomer; (b) the D_{6h} isomer.**TABLE 8: The Adiabatic and Vertical IPs and EAs of the Two Isomers (eV)**

isomer	parameter		result (eV)				
			HF	LDA	GGA	B3LYP	B3PW91
D _{2d}	IP	adiabatic	5.15	7.19	6.58	6.41	6.58
	vertical I		5.38	7.25	6.65	6.49	6.66
	vertical II		4.90	7.12	6.50	6.32	6.49
D _{6h}	EA	adiabatic	1.68	3.01	2.43	2.31	2.50
	vertical I		1.27	2.77	2.22	2.17	2.36
	vertical II		2.12	3.12	2.53	2.46	2.64
D _{6h}	IP	adiabatic	7.16	7.50	6.91	6.70	6.89
	vertical I		7.31	7.57	6.98	6.77	6.97
	vertical II		7.01	7.43	6.84	6.62	6.81
EA	adiabatic		0.28	3.25	2.66	2.50	2.67
	vertical I		0.18	3.18	2.58	2.43	2.59
	vertical II		0.38	3.33	2.74	2.58	2.75

Our LDA adiabatic EAs for the two isomers agree with those by Grossman et al.⁹ Recently, Kietzmann et al.⁷ measured the PES of the C₃₆ anion. From their PES, we can estimate the vertical EA (type II) of C₃₆ to be 2.8 eV, which is in good agreement with our calculated values for the D_{6h} isomer.

The energy gaps between the highest occupied and lowest unoccupied molecular orbitals (HOMO-LUMO) of the neutral isomers are listed in Table 9. Although the two isomers have roughly the same HOMO-LUMO gap, the gap size strongly depends on the computational methods. The HF method gives the biggest gap, whereas the LDA and GGA methods predict the smallest gaps. Our LDA and GGA results agree well with those calculated by Grossman et al.⁹ The DFT HOMO-LUMO gap has been successfully compared with the energy difference between the first excited state and the ground state for molecules and clusters.²⁶ Nevertheless, from the results in Table 9 one

TABLE 9: The HOMO–LUMO and QP Gaps (eV) of the Two Isomers

isomer	parameter	result (eV)					ref 9
		HF	LDA	GGA	B3LYP	B3PW91	
D _{2d}	HOMO–LUMO	5.74	0.42	0.42	1.39	1.39	0.4
	QP	3.47	4.18	4.15	4.10	4.08	
D _{6h}	HOMO–LUMO	6.42	0.46	0.48	1.42	1.46	0.5
	QP	6.88	4.25	4.25	4.20	4.22	

can see that none of our calculated gaps can match the experimental estimation of 0.8 eV.^{7,8} Kietzmann et al.⁷ estimated a gap of 0.8 eV for the C₃₆ molecule from their PES measurement, but they admitted this estimation was obtained with a large experimental error (~ 0.4 – 0.5 eV). There are two uncertainties in Collins et al.'s STS experiment,⁸ which make direct comparison between theory and experiment unlikely. The first is that it is not certain whether the STS measurement is performed on the individual C₃₆ molecules, and the second is that single electron tunneling effects may exist in the experiment that will result in an enlarged gap.²⁷

The quasiparticle (QP) energy gaps for the isomers are also listed in Table 7. The QP gap of a cluster can be rigorously defined as the energy difference between its adiabatic IP and EA within the Δ -self-consistent-field method.^{20,28} A remarkable result for the QP gaps is that all the DFT methods give almost the same value, quite different from the case for the calculated HOMO–LUMO gaps. The DFT QP gap of the D_{6h} C₃₆ isomer is ~ 4.2 eV, which is less than that of C₆₀ (~ 5.2 eV²⁰).

Finally, we calculate the molecular densities of states (DOS) of the two isomers. The DOS are obtained by Lorentzian extensions of the discrete energy levels and a summation over them. The broadening width parameter is chosen to be 0.1 eV. The DOS curves by LDA and GGA are very similar, and the DOS curves by B3LYP and B3PW91 are very similar. Therefore, we only plot the DOS curves by LDA and B3LYP in Figure 3. Although we can see sharp features in DOS from Figure 3, we cannot compare them directly with the experimental STS⁸ for the reason already mentioned. To understand the DOS, further state-of-the-art experiments are needed.

Summary

We conducted a comprehensive study of the structural and electronic properties of C₃₆ molecules with two most probable geometries (D_{6h} and D_{2d}), using the first-principles HF, LDA, GGA, B3LYP, and B3PW91 methods. The results we obtained can be summarized as follows.

(1) The geometry optimizations, performed on the singlet and triplet states of the two isomers, indicate that the ground state of the D_{6h} isomer depends on the computational methods. The triplet state is the ground state in the HF, B3LYP, and B3PW91 calculations, whereas the singlet state is the ground state in the LDA and GGA calculations.

(2) The ground state of the D_{2d} isomer, the singlet state, has almost the same energy as that of the D_{6h} isomer.

(3) Study of the relative stability of the two isomers in the charge states revealed that the D_{6h} anion is more stable than the D_{2d} anion, whereas the D_{2d} cation is lower in energy than the D_{6h} cation.

(4) The experimental fact that the C₃₆ molecule in the solid has D_{6h} symmetry is explained by the results of the relative stability of ionic isomers. The possible D_{2d} C₃₆ molecules, ions, and solids were predicted.

(5) The vibrational frequencies, IPs, EAs, HOMO–LUMO and QP gaps, and DOS were calculated for the two isomers.

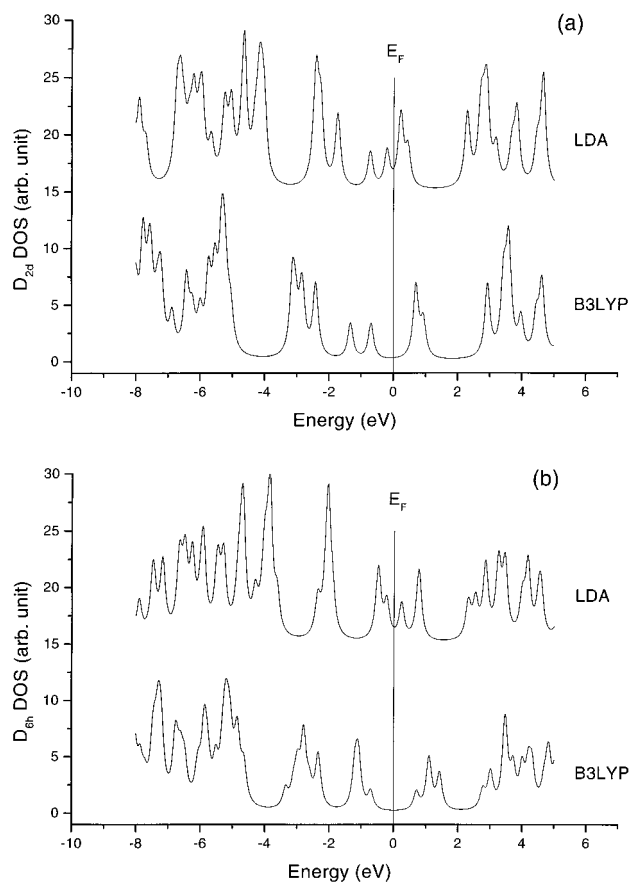


Figure 3. The DOS of C₃₆ by LDA and B3LYP: (a) the D_{2d} isomer; (b) the D_{6h} isomer.

These data are discussed and compared with the available experimental measurements.

Acknowledgment. This work was partially supported by the National Project for the Development of Key Fundamental Sciences in China, by the National Natural Science Foundation of China, by the Foundation of Ministry of Education of China, by the National High-Tech ICP committee in China, and by the Foundation of the Chinese Academy of Science. The HPCC, NSC, and SC&CG Laboratory of USTC are acknowledged for computational facilities.

References and Notes

- (1) Kroto, H. W.; Heath, J. R.; O'Brien, S. S.; Curl, R. F.; Smalley, R. E. *Nature* **1985**, *318*, 162.
- (2) Krätschmer, W.; Lamb, L. D.; Fostiropoulos, K.; Huffman, D. R. *Nature* **1990**, *347*, 354.
- (3) Piskoti, C.; Yarger, J.; Zettl, A. *Nature* **1998**, *393*, 771.
- (4) Heath, J. R. *Nature* **1998**, *393*, 730.
- (5) Fowler, P. W.; Mitchell, D.; Zerbetto, F. *J. Am. Chem. Soc.* **1999**, *121*, 3218.
- (6) Côte, M.; Grossman, J. C.; Cohen, M. L.; Louie, S. G. *Phys. Rev. Lett.* **1998**, *81*, 697.
- (7) Kietzmann, H.; Rochow, R.; Ganteför, G.; Eberhardt, W.; Vietze, K.; Seifert, G.; Fowler, P. W. *Phys. Rev. Lett.* **1998**, *81*, 5378.
- (8) Collins, P. G.; Grossman, J. C.; Côte, M.; Ishigami, M.; Piskoti, C.; Louie, S. G.; Cohen, M. L.; Zettl, A. *Phys. Rev. Lett.* **1999**, *82*, 165.
- (9) Grossman, J. C.; Côte, M.; Louie, S. G.; Cohen, M. L. *Chem. Phys. Lett.* **1998**, *284*, 344.
- (10) Slanina, Z.; Zhao, X.; Ōsawa, E. *Chem. Phys. Lett.* **1998**, *290*, 311.
- (11) Halac, E.; Burgos, E.; Bonadeo, H. *Chem. Phys. Lett.* **1999**, *299*, 64.
- (12) Fowler, P. W.; Heine, T.; Rogers, K. M.; Sandall, J. P. B.; Seifert, G.; Zerbetto, F. *Chem. Phys. Lett.* **1999**, *300*, 369.
- (13) Jagadeesh, M. N.; Chandrasekhar, J. *Chem. Phys. Lett.* **1999**, *305*, 298.

- (14) *Gaussian 94, Revision B.1*; Frisch, M. J.; Trucks, G. W.; Schlegel, H. B.; Gill, P. M. W.; Johnson, B. G.; Robb, M. A.; Cheeseman, J. R.; Keith, T.; Petersson, G. A.; Montgomery, J. A.; Raghavachari, K.; Al-Laham, M. A.; Zakrzewski, V. G.; Ortiz, J. V.; Foresman, J. B.; Cioslowski, J.; Stefanov, B. B.; Nanayakkara, A.; Challacombe, M.; Peng, C. Y.; Ayala, P. Y.; Chen, W.; Wong, M. W.; Andres, J. L.; Replogle, E. S.; Gomperts, R.; Martin, R. L.; Fox, D. J.; Binkley, J. S.; Defrees, D. J.; Baker, J.; Stewart, J. P. Head-Gordon, M.; Gonzalez, C.; Pople, J. A. Gaussian, Inc.: Pittsburgh, PA, 1995.
- (15) Vosko, S. H.; Wilk, L.; Nusair, M. *Can. J. Phys.* **1980**, *58*, 1200.
- (16) Perdew, J. P.; Wang, Y. *Phys. Rev. B* **1992**, *45*, 13244.
- (17) Becke, A. D. *J. Chem. Phys.* **1990**, *98*, 5648.
- (18) Lee, C.; Yang, W.; Parr, R. G. *Phys. Rev. B* **1988**, *37*, 785.
- (19) Szabo, A.; Ostlund, N. S. *Modern Quantum Chemistry*; Macmillan: New York, 1982; pp 180–190.
- (20) Cappellini, G.; Casula, F.; Yang, Jinlong; Bechstedt, F. *Phys. Rev. B* **1997**, *56*, 3628.
- (21) Kobayashi, K.; Kurita, N.; Kumahara, H.; Tago, K.; Ozawa, K. *Phys. Rev. B* **1992**, *45*, 13690.
- (22) Grossman, J. C.; Louie, S. G.; Cohen, M. L. *Phys. Rev. B* **1999**, *60*, 6941.
- (23) Pearson, R. G. *J. Am. Chem. Soc.* **1969**, *91*, 1252.
- (24) Fowler, P. W.; Sandall, J. P. B. *J. Chem. Soc., Perkin Trans. 2* **1994**, 1917.
- (25) Jishi, R. A.; Dresselhaus, M. S. *Chem. Phys. Lett.* **1999**, *302*, 533.
- (26) Jones, R. O.; Gunnarson, O. *Rev. Mod. Phys.* **1989**, *61*, 689.
- (27) Banin, U.; Cao, Y. W.; Katz, D.; Millo, O. *Nature* **1999**, *400*, 542.
- (28) Godby, R. W.; Schlüter, M.; Sham, L. J. *Phys. Rev. B* **1988**, *37*, 10159.